JOURNAL OF BIOMEDICAL OPTICS 4(1), 85–93 (JANUARY 1999)

OPTICAL DIAGNOSTICS OF MECHANICAL PROPERTIES OF RED BLOOD CELLS BASED ON THE DEFORMATION BY HIGH FREQUENCY ELECTRIC FIELD

V. L. Kononenko and T. A. Ilyina
Institute of Biochemical Physics, Russian Academy of Sciences, Kosygin Street 4, 117977 Moscow, Russia

(Paper JBO/ODB-003 received Jan. 1, 1998; revised manuscript received Nov. 19, 1998; accepted for publication Nov. 25, 1998.)

ABSTRACT

Erythrocyte placed in a low-conductivity isotonic medium can be elongated by a high frequency electric field. The elongation can be registered optically, finally enabling the determination or monitoring of elastic moduli and viscous properties of erythrocytes. However, an unambiguous evaluation of mechanical parameters from the optical data is complicated. It requires an adequate theory of dielectro deformation which takes into account the influence of the cell's mechanical, electric, and transient shape parameters on field-induced deformations. The present work is aimed at the development of a comprehensive and experimentally verified theoretical basis for the dielectro-deformational investigation of erythrocytes. The previous concept of the dielectro-deformation process, supported solely by the shear deformation of erythrocyte membrane, is revised completely. It is shown that in the practical relevant range of dielectro deformation, it is mainly supported by bending deformation of the membrane, with a gradual development of shear deformation as the cell becomes more elongated. This new bending-shear theory of dielectro deformation is developed here. The theory is shown to describe unambiguously both observational and quantitative data on the static and dynamic dielectro deformation of erythrocytes. [S1083-3668(99)01701-3]

Keywords erythrocytes; mechanical properties; optical diagnostics.

1 INTRODUCTION

It is well established now that mechanical properties of erythrocytes can be used as a good indicator of the physiological state and various pathological transformations both in the circulatory system and in the entire organism.[1] Several rheological techniques based on this approach have been developed and used for biomedical diagnostics.[2–4] However, the necessity for new techniques still exists, especially for those combining a wide dynamical range of deformation values and flexibility in the time pattern of the deformation process. Such possibilities are offered by a novel technique—the optically registered dielectro deformation of cells.[5–10] The technique is based on a fundamental physical phenomenon: a polarizable body, surrounded by a less polarizable medium, tends to become elongated in the direction of the electric field applied. The elongation is quadratic in field strength, because the acting force is proportional to the product of the field strength and the density of the polarization charge induced, the latter also being proportional to the field strength. Hence, even in an alternating field, there exists a stationary component of cell elongation. Actually, for such viscous objects as erythrocytes, for so high a basic frequency of electric field, usually in the megahertz range, this is the only observable deformation component. However, if the field amplitude is also varied in the low frequency range according to some time pattern, it induces dynamic deformations in the cell and can be used to achieve the desired time course of deformation.

The main problem in the practical implementation of the dielectro-deformational technique is the establishing of correct relations between the deformations observed and the mechanical, electrical, and geometrical parameters of erythrocyte. The original theory of the dielectro deformation of erythrocytes[6] did not take into account several basic features of the deformation process: it completely ignored the contribution to cell elongation from bending deformations of the cell membrane; it considered the initial cell shape to be spherical instead of a discoid one; it neglected the strict conservation condition for the membrane area, and an actual conservation condition for the cell volume during the deformation; it neglected the dependence of the

Address all correspondence to Dr. Vadim Kononenko. Fax: (7-095)-137-41-01; E-mail: konon@glasnet.ru

1083-3668/99/$10.00

actual value of the electric force on the transient cell shape. It is shown[10] that such radical oversimplifications make this theory unacceptable for a quantitative description of the deformational curves measured, and may even lead to misinterpretation of the observations.

In principle, the dielectro-deformation problem can be solved rigorously on the basis of cell biomechanics equations[2] and the theory of ponderomotive action of the electric field.[11,12] However, due to the complex shape of the erythrocyte, a complicated numerical procedure, which should be repeated successively for each instantaneous value of the field amplitude in the case of the dynamic dielectro-deformations, is required. As a result, such a rigorous theory may exist, distributed and used in the form of a complicated computer program only (which, from the general point of view, is a straightforward and very promising trend in modern science). A reasonable alternative to such an approach, one that turned out to be very productive, is the three-axis ellipsoid approximation for the shape of human erythrocyte suggested in Ref. 8. Using this approximation, it is possible to derive a rather simple analytical equation of dielectro deformations, and even obtain analytical solutions (for static and for some dynamic deformations).[8,10]

In this article this approach is used to incorporate the analysis of bending deformation of an erythrocyte membrane into theory, and to obtain the general dynamic equation of dielectro deformations. The theory is verified by comparing it with existing experimental results both on static and dynamic dielectro deformation of erythrocytes. The shape of the erythrocyte is modeled by a three-axis ellipsoid with the semi-axis a parallel to the direction of the homogeneous external high-frequency electric field, and semi-axes b and c perpendicular to this field. At zero field strength it is an oblate spheroid with $a=b\gg c$. It is known that the surface area S of the erythrocyte remains constant under physiologically tolerable deformations.[2] It is reasonable to assume also that the erythrocyte does not change its volume V during dielectro deformation. Mathematically, the shape of the ellipsoid, with constant volume and surface area, can be described by a single parameter, a convenient choice being the axes ratio $\kappa=a/b\geq 1$. This ratio will be the basic shape variable both in the measuring procedures analyzed in this article and in the dielectro-deformation theory developed.

2 REGISTRATION TECHNIQUES

Two basic experimental arrangements are used for optical diagnostics of erythrocytes by means of dielectro deformation. To test the individual cell properties, either microphotometering of a single cell[5,8] or TV image processing[6] is employed. To obtain the population-average characteristics, laser diffractometry of an erythrocyte suspension in a flow was used.[7] In both arrangements, one of the main problems is the proper choice of the quantities measured and establishing their relationship to the cell deformation parameters. As follows from the ellipsoidal approximation, deformation of the erythrocyte in the electric field should be characterized by the ratio κ of the longitudinal and transverse dimensions of the cell, rather than by the absolute value of its elongation. If cell image processing is used,[6] this ratio can be obtained directly. If laser diffractometry is used,[7] this ratio can be determined by image processing of the diffraction pattern because, for an ellipse, this pattern is a set of elliptical rings exactly the same axes ratio, but rotated 90°.[13]

The situation is more complicated if the microphotometering of a single cell is carried out using phase-contrast[5,8] or absorption microscopy. Consider first the latter procedure as being more straightforward. Here the registered quantity is the total light intensity passing through the measuring diaphragm, usually of rectangular shape, with dimensions $l\times h$ of its projection at the cell surface. The fraction of light intensity absorbed by the cell is proportional to its local thickness integrated over the part of the cell contour inside the diaphragm projection. This integral is, evidently, the part of the cell volume contained within (or cut by) this projection. If the projection rectangle exceeds the cell contour, then no signal variation due to cell elongation should be expected, because the cell volume does not change during this process. Hence, in order to obtain the signal variation, one of the side dimensions, say, h, of the diaphragm projection should be taken as small compared to the cell size. Let i_0 be the light flux density at the object plane of the microscope, α the absorption coefficient of the cell material, and the diaphragm projection with $l>2a$ and $h<2b$ be positioned symmetrically along the a axis of the ellipsoid-shaped cell. Then the total light intensity $I(\kappa)$ passing through the measuring diaphragm can be shown to be

$$I(\kappa)=i_0\left[lh-\alpha\pi ha(\kappa)c(\kappa)\left(1-\frac{h^2}{12b(\kappa)^2}\right)\right]. \quad (1)$$

If $h>2b$, then h should be replaced by $2b$ in the second term in square brackets in Eq. (1) which we denote as $\Delta I(\kappa)$. That gives $\Delta I(\kappa)=-\alpha 4\pi/3abc$ being proportional to the constant volume of the cell ellipsoid.

A similar relationship can be established for the phase-contrast regime of microphotometering. If the phase shift $\varphi(x,y)=n_r d(x,y)$ introduced by the cell is small compared to unity, then the light intensity distribution in the object plane of a phase-contrast microscope is described by[13]

$$i(x,y)=i_0[A^2\pm 2A\varphi(x,y)]. \quad (2)$$

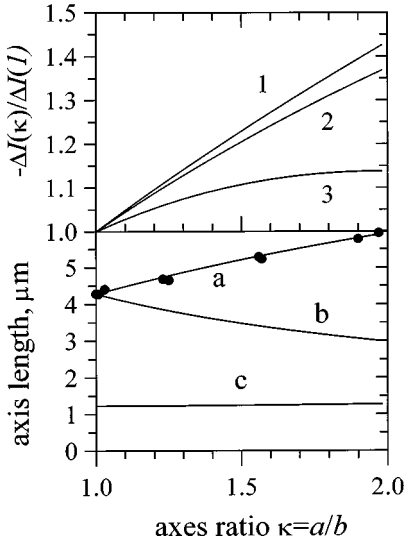

Fig. 1 Top dependence of the varying part $\Delta I(\kappa)$ of the light flux through the measuring diaphragm on the cell axes ratio κ, calculated for various diaphragm widths: $h=1$ (1), 3 (2), and 6 μm (3); bottom: dependence of the absolute length of cell axes on κ, calculated for an ellipsoidal model with $S=134.1\ \mu\text{m}^2$ and $V=94.1\ \mu\text{m}^3$. The circles denote half of the cell elongation determined by processing the erythrocyte images in Ref. 6.

Here n_r is the relative refraction index of the cell material, $d(x,y)$ is the local cell thickness, A is the transmission coefficient of the phase plate in the microscope objective, and $(\pm)$ stands for the phase lag/lead introduced by the phase plate. It is clear from Eq. (2) that $2An_r$ plays the role of absorption coefficient α in Eq. (1), leading to a similar expression for the total registered light intensity.

Hence, to obtain the actual value of the cell axes ratio κ from the microphotometering data, it is necessary to know the dependencies $a(\kappa)$, $b(\kappa)$, and $c(\kappa)$. They can be obtained numerically for the cell ellipsoid, provided its volume and surface area are known (or measured independently). These dependencies are shown at Figure 1 together with the corresponding dependence of the varying part $\Delta I(\kappa)$ of light intensity (1) passing through the measuring diaphragm. Both the absolute elongation of the erythrocyte (i.e., the a axis) and $\Delta I(\kappa)$ depend essentially nonlinearly on the cell axes ratio. However, this nonlinearity is small for $\kappa<1.5$ and $h \ll 2b$, as Figure 1 shows. That allows the direct use of the registered field dependencies of a or ΔI for a description of those dynamic dielectro deformations, where only the shape of the kinetic curves is essential (see, e.g., Refs. 6 and 8). On the other hand, evaluation of stationary dielectro deformations, where the absolute deformation value is of interest, requires the use of the exact relation between the microphotometer signal and the cell axes ratio, hence, knowledge of S and V.

It should be emphasized here that, regardless of whether the measuring procedure does or does not require knowledge of the cell volume and surface area, these quantities are nevertheless necessary for further evaluation of cell mechanical moduli from the deformation values obtained.

Additional details of the measurement procedures can be found elsewhere.[6,8]

3 THEORY OF DIELECTRO DEFORMATIONS

Consider an erythrocyte placed in a homogeneous high-frequency electric field $E=E(t)\exp(j\omega t)$, where ω is the basic field frequency, j is the imaginary unit, and $E(t)$ is a slowly varying field amplitude. According to Ref. 2, an erythrocyte is considered to be a thin viscoelastic shell (cell membrane) filled with viscous fluid (hemoglobin solution). Mechanical properties of the cell membrane are characterized by the shear elastic modulus μ, bending elastic modulus K_c, and surface viscosity η_s. In the general case of dynamic deformations, the transient shape of a cell is determined by the instantaneous mechanical equilibrium between all forces applied to the membrane, namely, the ponderomotive force F_p from the external electric field and mechanical forces arising in the membrane due to its deformation: shear elastic force F_e, bending stiffness force F_b, membrane internal friction force F_{ds}, and volume viscous drag force F_{dv}. The inertia forces can be neglected due to the very small thickness of the cell membrane and the slow nature of the practically implemented deformations. In principle, the force's equilibrium condition should be applied to every small membrane element, leading to a complicated set of integrodifferential equations. However, use of the ellipsoidal approximation for the cell shape together with the $V,S=\text{const}$ enables one to introduce the corresponding generalized forces, which are related to the entire membrane and depend on a single variable only—the shape parameter κ.[8,10] Then the condition of mechanical equilibrium takes the form

$$F_p(\kappa,t)+F_e(\kappa)+F_b(\kappa)+F_{ds}\left(\kappa,\frac{d\kappa}{dt}\right)+F_{dv}\left(\kappa,\frac{d\kappa}{dt}\right)=0. \tag{3}$$

The expressions for the generalized forces F_p, F_e, and F_{ds} were obtained elsewhere:[8]

$$F_p(\kappa,t)=VF(\omega)|\chi(\omega,\kappa)|^2\left|\frac{\partial N_a}{\partial\kappa}(\kappa)\right|E(t)^2,$$

$$F_e(\kappa)=-\frac{1}{2}S\mu\left(1-\frac{1}{\kappa^2}\right), \tag{4}$$

$$F_{ds}\left(\kappa,\frac{d\kappa}{dt}\right)=-S\eta_s\frac{1}{\kappa^2}\frac{d\kappa}{dt}.$$

Here $F(\omega)$ is the frequency factor of the ponderomotive force, the function $\chi(\omega,\kappa)$ relates the field

amplitude inside the cell $E^{(i)}(\omega,\kappa,t)$ to the applied field amplitude as $E^{(i)}(\omega,\kappa,t)=\chi(\omega,\kappa)E(t)$, and $N_a(\kappa)$ is the depolarization factor[11] of the ellipsoid associated with its a axis. According to Ref. 8,

$$F(\omega)=\frac{\varepsilon_e}{16\pi}\frac{\left(\frac{\varepsilon_i}{\varepsilon_e}-1\right)^2(\omega\tau_e)^2+\left(\frac{\sigma_i}{\sigma_e}\right)^2-2\frac{\varepsilon_i}{\varepsilon_e}+1}{1+(\omega\tau_e)^2},$$
$$\tau_e=\frac{\varepsilon_e}{4\pi\sigma_e}, \tag{5}$$

where $\varepsilon^{(k)}(\omega)=\varepsilon_k-j4\pi\sigma_k/\omega$ are complex dielectric permittivities of internal hemoglobin solution ($k=i$) and of surrounding medium ($k=e$), respectively. The particular form of $\chi(\omega,\kappa)$ depends on the specific electrical model of the cell. As was shown previously,[8] in the frequency range used for dielectro deformations, the contribution by the membrane to electrical properties of the erythrocyte can be neglected, and the following expression can be used:

$$\chi(\omega,\kappa)=\frac{\varepsilon^{(e)}(\omega)}{[\varepsilon^{(i)}(\omega)-\varepsilon^{(e)}(\omega)]N_a(\kappa)+\varepsilon^{(e)}(\omega)}. \tag{6}$$

The bending stiffness force F_b was not even considered in the previous theories reported.[6,10] It was supposed *a priori* that the cell elongation in the electric field is too large to be supported by bending deformation of the membrane; hence, it is due completely to shear deformation. However, the phase-contrast cell images presented in Figure 2 of Ref. 6 show quite distinctly that the erythrocyte keeps its biconcave shape up to elongations of $\kappa\approx1.9$. It is known that the biconcave shape results from the distribution of rather weak bending rigidity forces over the membrane under zero shear stress.[2] The latter is due to the excess in the membrane area and to a very high shear elastic modulus value compared to that of the bending one. Hence, the observations reported in Ref. 6 indicate that the initial, and even rather developed, stages of cell elongation are supported by the change of the membrane curvature. At the initial stages, no or minor shear deformations of the membrane are required to support the elongation. Hence, the shear elastic forces that arise are very small. Only when nearing the limit of the elongation by means of a curvature change do shear deformations start to develop. Mathematically, that means the κ value in expressions (4) for $F_e(\kappa)$ and $F_{ds}(\kappa,d\kappa/dt)$ cannot be the cell axes ratio. It should be replaced by some effective value $\kappa^*(\kappa)$ describing the actual shear deformation of the membrane element at the given axes ratio. Evidently, it is impossible to obtain an exact analytical expression for $\kappa^*(\kappa)$, even in the framework of the ellipsoidal approximation. However, using some obvious general requirements for the functional behavior of $\kappa^*(\kappa)$, various interpolating analytical expressions can be constructed. The requirements for these are $\kappa^*(1)=1$ in the nondeformed state, $\kappa^*(\infty)=\kappa$ at very large elongations, and the analytical possibility to control the transition region from predominantly bending to completely shear deformations. A simple and convenient interpolation law is as follows:

$$\kappa^*(\kappa)=1+\frac{\kappa-1}{\left(\frac{w}{\kappa-1}\right)^n+1}. \tag{7}$$

Here w and n are adjustable parameters to be determined from the experiment. The first characterizes an effective width of κ range, where the transition from the bending to the shear deformations of the membrane occurs. The second parameter characterizes the steepness of this transition.

A generalized bending stiffness force $F_b(\kappa)$ can be introduced using the same procedure as that for the other generalized forces acting on the erythrocyte membrane.[8] The membrane bending energy is described by the well known Helfrich expression:

$$W_b=\frac{K_c}{2}\int(C_1+C_2-C_0)^2\,dS. \tag{8}$$

Here C_1 and C_2 are two principal local curvatures of the membrane element dS, and C_0 is the spontaneous curvature of the membrane.[2] For an ellipsoidal shell with $V,S=\text{const}$, the bending energy, Eq. (8), depends on the axes ratio κ only. Hence, $F_b(\kappa)$ can be defined as the negative κ derivative from $W_b(\kappa)$. An exact $F_b(\kappa)$ dependence can be obtained from Eq. (8) using the standard formulas for the curvature of the ellipsoid, but in numerical form only. To get an approximate analytical expression, we consider an ellipsoidal surface as consisting of two parts where the local curvatures have their specific but coordinate-independent values. Hence the cell is modeled by a very oblate ellipsoid (Figure 1); it is easy to distinguish the central part that consists of two segments of the ellipsoid, and the circumferential, or the rim, part of the cell. The central part of area $2S_1$ has low, nearly equal principal curvatures, while the rim part of area S_2 has two essentially different principal curvatures. With further approximation, the relevant curvature values can be identified with the principal curvatures at the ellipsoid poles associated with the a, b, and c axes. The latter curvatures are

$$a\ \text{axis:}\ C_{1a}(\kappa)=\frac{a}{b^2},\ C_{2a}(\kappa)=\frac{a}{c^2},$$
$$b\ \text{axis:}\ C_{1b}(\kappa)=\frac{b}{a^2},\ C_{2b}(\kappa)=\frac{b}{c^2}, \tag{9}$$

$$c \text{ axis: } C_{1c}(\kappa)=\frac{c}{a^2},\ C_{2c}(\kappa)=\frac{c}{b^2}.$$

The approximations adopted reduce the integration in Eq. (8) to the summation over two parts of the ellipsoid surface defined above. Using Eqs. (9), we obtain

$$W_b(\kappa)\simeq\frac{K_cS}{2(1+q)}\left[q\left(\frac{c}{a^2}+\frac{c}{b^2}-C_0\right)^2+\frac{1}{2}\left(\frac{a}{b^2}+\frac{a}{c^2}-C_0\right)^2+\frac{1}{2}\left(\frac{b}{a^2}+\frac{b}{c^2}-C_0\right)^2\right],$$

$$F_b(\kappa)=-K_cf_b(\kappa),\ f_b(\kappa)=S\frac{dW_b(\kappa)}{d\kappa}. \qquad (10)$$

Here $q=2S_1/S_2$, and $2S_1+S_2=S$. Assuming the boundary line between the central part S_1 and the rim part S_2 of the cell to be the line of maximum erythrocyte thickness, we can obtain an estimate of $q=1.4$. The spontaneous curvature C_0 value is determined by the minimum condition for the bending energy at $\kappa=1$, or $F_b(1)=0$. Analytical expressions for dimensionless function $f_b(\kappa)$ and for C_0 are easily obtained. They were used in the numerical calculations, but are not shown here because they are lengthy.

A lesser contribution by the membrane shear deformations to the actual cell elongation also leads to a decrease in the viscous energy dissipation in the membrane during the dynamic deformations. Under these conditions, the energy dissipation inside the internal hemoglobin solution and in the surrounding medium cannot be further neglected. The corresponding viscous drag force F_{dv} can be introduced through the dissipation function using the approach described in Ref. 8. In the general form this force can be written as follows:

$$F_{dv}\left(\kappa,\frac{d\kappa}{dt}\right)=-V\eta_if_{dv}(\kappa,\eta_i,\eta_e)\frac{d\kappa}{dt}. \qquad (11)$$

Here $f_{dv}(\kappa,\eta_i,\eta_e)$ is a dimensionless function, and η_i and η_e are viscosity coefficients of the hemoglobin solution and the surrounding medium, respectively. In exact form $f_{dv}(\kappa,\eta_i,\eta_e)$ can be obtained only numerically. However, an approximate analytical expression can be derived using simple physical arguments. As Figure 1 shows, $c(\kappa)\simeq\text{const}\ll a,b$ for $\kappa<2$. Hence, to evaluate the viscous energy dissipation, we consider the erythrocyte as a very thin circular disk which transforms under field action into an elliptical disk. The transformation proceeds under the constant area of the disk faces, with some characteristic velocity $d\kappa/dt$. It can be considered to be a time-dependent linear scale transformation along the a and b axes. The corresponding two-dimensional velocity distribution is easily obtained from the transformation law: $v_x=(x/2\kappa)d\kappa/dt$, $v_y=-(y/2\kappa)d\kappa/dt$. This velocity distribution gives the components of the viscous stress tensor, and knowing these enables one to calculate the rate of energy dissipation[14] inside the hemoglobin solution. The rate of energy dissipation outside the cell can be evaluated as the product of the characteristic velocity of the cell edge displacement during deformation and the viscous drag force that arises. The latter force expression is available for a thin circular disk.[14] By summing the internal and external energy dissipation terms, and by taking the velocity derivative of this sum, we obtain the following approximate expression for the dimensionless function $f_{dv}(\kappa,\eta_i,\eta_e)$ entering into Eq. (11):

$$f_{dv}(\kappa,\eta_i,\eta_e)=\left(1+\frac{S^{3/2}}{6\pi^{3/2}V}\cdot\frac{\eta_e}{\eta_i}\right)\frac{1}{\kappa^2}. \qquad (12)$$

Substituting into force balance Eq. (3) the generalized forces expressions (4) and (10)–(12), with $\kappa^*(\kappa)$, Eq. (7), replacing κ in $F_e(\kappa)$ and $F_{ds}(\kappa,d\kappa/dt)$, we finally obtain

$$-\frac{d\kappa}{dt}=\left[\frac{\tau_0}{(\kappa^*)^2}\frac{d\kappa^*}{d\kappa}+\frac{\tau_1}{\kappa^2}\left(1+\frac{S^{3/2}}{6\pi^{3/2}V}\frac{\eta_e}{\eta_i}\right)\right]^{-1}\times\left[\frac{K_c}{\mu S}f_b(\kappa)+\frac{1}{2}\left(1-\frac{1}{(\kappa^*)^2}\right)-F(\omega)|\chi(\omega,\kappa)|^2\left|\frac{\partial N_a}{\partial\kappa}(\kappa)\right|\frac{VE(t)^2}{\mu S}\right],$$

$$\kappa^*(\kappa)=1+\frac{\kappa-1}{\left(\frac{w}{\kappa-1}\right)^n+1}. \qquad (13)$$

Here $\tau_0=\eta_s/\mu$ and $\tau_1=\eta_iV/\mu S$ are effective times of viscoelastic relaxation of the membrane due to the energy dissipation in the membrane material and hemoglobin solution, respectively.

Equation (13) is the general dynamic equation for dielectro deformations of erythrocytes based on the bending-shear ellipsoidal model. The first and the second terms in the second set of square brackets describe the contributions by the bending and the shear deformations, respectively. They are determined by essentially different characteristic amplitudes because the factor $K_c/\mu S\ll 1$ (e.g., $\simeq 10^{-3}$ for human erythrocytes). Hence, these contributions are comparable only if $\kappa^*-1\ll\kappa-1$, which requires $w\gg\kappa-1$ and $n>0$ in Eqs. (7) and (13). For the practically relevant deformation range, $\kappa<2$; that means $w\gg 1$. In the limit of $w\to 0$, which means the onset of shear deformation only from the beginning of cell elongation, $\kappa^*(\kappa)\to\kappa$, and Eq. (13) transforms into the dielectro-deformation equation obtained earlier for the purely shear model.[8] Hence, the main qualitative features of Eq. (13) are similar to those analyzed in Refs. 8 and 10. In particular,

the dependence of the force factor $F(\omega)|\chi(\omega,\kappa)|^2$ on the basic field frequency ω is exactly the same as that described in Refs. 8 and 10. Another feature, and a very important one, is that cell elongation depends on the field amplitude $E(t)$ indirectly through the dimensionless combination $(V/\mu S)^{1/2}E(t)$. That means that a quantitative evaluation of the cell mechanical moduli from the deformation curves registered requires knowledge of the geometrical parameters of erythrocyte, at least, its volume and membrane area values.

4 EXPERIMENTAL VERIFICATION

Validation of the adequacy of the bending-shear model of dielectro deformations should begin by a validity check of the ellipsoidal approximation for the shape of a deformed erythrocyte. Figure 2 of Ref. 6 presents a series of phase-contrast images of a single erythrocyte in different stages of elongation in a high-frequency electric field. These images show that for moderate elongations (up to $\kappa \approx 2$) the cell contour is close to an ellipse, while at higher field strengths a tip develops at the cell edge pointing toward the field direction. The images here were processed to give the experimental dependence between the axis ratio κ and the absolute cell elongation, shown in Fig. 1. The theoretical dependencies $a(\kappa)$, $b(\kappa)$, $c(\kappa)$ were calculated for the statistical-average values of the surface area and volume of human erythrocyte $S=134.1\,\mu\text{m}^2$, and $V=94.1\,\mu\text{m}^3$, taken from Ref. 2. The close correspondence between the observed and the calculated cell elongation in the range $\kappa \leqslant 2$ justifies the use of the three-axis ellipsoidal approximation for the shape of erythrocytes.

4.1 STATIONARY DEFORMATIONS

The stationary deformations of erythrocytes are accomplished using a high-frequency electric field with constant amplitude. That corresponds to $E(t)=E=\text{const}$ and $d\kappa/dt=0$ in general Eq. (13). Using the stationary deformation equation thus obtained, the cell elongation curves $\kappa(E)$ were calculated for various relative contributions by the bending and the shear deformation of the membrane (Figure 2). In the model used, these contributions are determined by two parameters in Eqs. (7) and (13), w and n. For purely bending deformations $w=\rightarrow\infty$, whereas for purely shear deformations $w=0$. The functional dependence of depolarization factor $N_a(\kappa)$ was calculated using standard expressions[11] and was approximated by a polynomial. The electrical parameters used for the calculation of $F(\omega)$ and $\chi(\omega,\kappa)$, the elastic moduli, and the geometrical parameters of erythrocyte were as follows for all theoretical curves in this article: $(\omega/2\pi)=1$ MHz, $\varepsilon_i=60$, $\sigma_i=0.4$ S/m, $\varepsilon_e=80$, $\sigma_e=0.01$ S/m, $\mu=6.1\times10^{-6}$ N/m, $K_c=1.8\times10^{-19}$ J, $S=134.1\,\mu\text{m}^2$, and $V=94.1\,\mu\text{m}^3$. The cup/rim area ratio of the erythrocyte in the elastic bending energy term in Eqs. (10) and (13) was estimated to be $q=1.4$ using the cell shape parameters from Ref. 2. The experimental curves shown in Figure 2 were obtained by processing the curves in Figure 3 of Ref. 6 based on the calculated dependence $a(\kappa)$ (see Figure 1) and on scaling the field amplitude to the dimensionless acting force $(V/\mu S)^{1/2}E$.

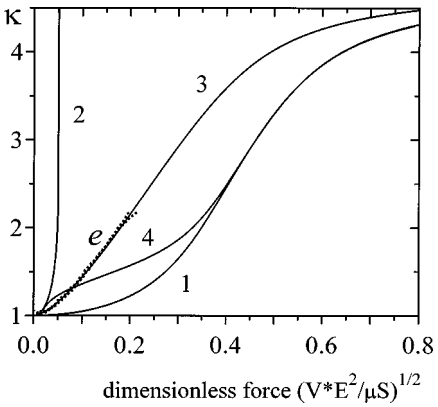

Fig. 2 Comparison of the measured elongation curves [(e), obtained by processing the data of Ref. 6] and the curves calculated using the shear (1), bending (2), and bending-shear (3), (4) models of dielectro deformations of the erythrocyte. $w=0$ for (1); $w\rightarrow\infty$ for (2); $w=110$, $n=0.45$ for (3); $w=0.75$, $n=3$ for (4).

The calculated deformation curves are essentially nonlinear and saturate at high values of $(V/\mu S)^{1/2}E$. The latter is a consequence of the condition $V,S=\text{const}$ holds for the erythrocyte during the deformation: the elongation of a body under constant volume and surface area cannot be indefinite due to the purely geometrical constraint. Assuming the final stage of elongation to be a thin cylinder with $\kappa \gg 1$, which gives the maximum estimate of the elongation, we get approximately $\kappa_{\max} \simeq (S^3/16\pi V^2)$. That gives $\kappa_{\max} \simeq 5.4$, while the exact calculation gives $\kappa_{\max}=5$. Curves (1) and (2) of Figure 2 show that neither purely bending nor purely shear deformations of erythrocyte membrane can describe the measured elongation curves. That means that the bending elastic stress that arises in a deformed membrane is too weak to balance the acting electric force. On the other hand, the shear elastic stress, which would correspond to the elongation observed, is excessively high in the scale of this force. As curve (3) shows, the actual deformation process is the predominant bending deformations at the beginning, with a very steep increase of shear deformations as the cell elongations increase. On the contrary, if the effective ranges of predominantly bending and predominantly shear deformations are well separated, which is described by smaller w and larger n, the elongation curve would have two corresponding characteristic parts [curve (4)]. The calculations give a good description of the curves measured in the parameter range $w=110\pm10$ and $n=0.45\pm0.02$. It should be noted that the

fitting of these parameters is related to the estimate $q=1.4$ made for the $2S_1/S_2$ ratio. Hence, it is a model-dependent set of parameters, sensitive to the choice of q.

These results show that the bending-shear model developed can be used successfully for quantitative evaluation of the stationary dielectro deformations of erythrocytes.

4.2 DYNAMIC DEFORMATIONS

The use of an appropriate time pattern $E(t)$ of the amplitude modulation of high-frequency electric field enables one, in principle, to accomplish any type of dynamic deformation of a cell desired. In practice, two types of amplitude modulation were used: stepwise[6] and low-frequency periodic[8] modulation. The main objective of such measurements is registration of the kinetics of viscoelastic relaxation of a deformed cell and determination of the characteristic effective time $\tau_0=\eta_s/\mu$ in Eq. (13), which enables one to monitor the membrane viscosity. Here we shall analyze a viscoelastic response of a cell to a field jump from E_0 to E_1 as the most direct way to determine τ_0. According to general Eq. (13), the effective time τ_{eff} governing the observed elongation or relaxation kinetics differs substantially from τ_0 and depends essentially on the initial cell elongation $\kappa_0=\kappa(E_0)$. This can be shown by considering very small jump amplitudes $|E_1-E_0| \ll E_0$. In this case we may put $\kappa=\kappa_0+\xi(t)$, $E=E_0+\Delta E(t)$ in Eq. (13), and make the linear expansions over $|\xi|\ll\kappa_0$ and $|\Delta E|\ll E_0$ of the functions involved. As a result, we obtain a standard relaxation-type differential equation for $\xi(t)$:

$$-\tau_{\text{eff}}(E_0)\frac{d\xi}{dt}=\xi-\frac{d\kappa_0}{dE}(E_0)\Delta E(t), \tag{14}$$

$$\tau_{\text{eff}}(E_0)=\left[\frac{\tau_0}{[\kappa^*(\kappa_0)]^2}\frac{d\kappa^*}{d\kappa}(\kappa_0)+\frac{\tau_1}{\kappa_0^2}\left(1+\frac{S^{3/2}}{6\pi^{3/2}V}\frac{\eta_e}{\eta_i}\right)\right]\frac{\mu S\frac{d\kappa_0}{dE}(E_0)}{2f_p(\kappa_0,\omega)VE_0}.$$

Here $f_p(\kappa,\omega)$ is the dimensionless function entering the expression for ponderomotive force, Eq. (4) as $F_p(\kappa,t)=Vf_p(\kappa,\omega)E(t)^2$. According to Eq. (14), for $\Delta E=\text{const}$ the dynamic component $\xi(t)$ varies exponentially, the effective relaxation time being $\tau_{\text{eff}}(E_0)$. This time is a combination of characteristic cell material times τ_0 and τ_1, and it strongly decreases with the increase of the initial cell elongation κ_0.

Figure 3 shows a comparison of the theoretical elongation curves, calculated according to Eq. (13) for the experimental conditions of Ref. 6, with the curve obtained by processing the experimental curve from Figure 3 of Ref. 6. The calculations were done for $\tau_0=0.12\,\text{s}$,[2] $\tau_1/\tau_0=0.3$, $w=110$, and $n=0.45$, and the rest of parameters are listed in the Sec. 4.1. (The ratio τ_1/τ_0 was used here as an adjustable parameter. Its correspondence with the estimate obtained from Eq. (13) is discussed at the end of Sec. 4.2.) First of all, this comparison demonstrates once again the inadequacy of the purely shear model[6,10] for a description of erythrocyte dielectro deformations. Second, it shows that general Eq. (13) describes both the stationary and the dynamic deformations well. Third, the theory explains the decrease of cell relaxation time with an increase of the initial field amplitude, observed experimentally.[6] The theoretical dependencies $\tau_{\text{eff}}(E)$ are shown in Figure 4 for various models. They were obtained from the slope in the log-log scale of the elongation kinetic curves calculated using Eq. (13) for the field jump conditions with $|E_1$

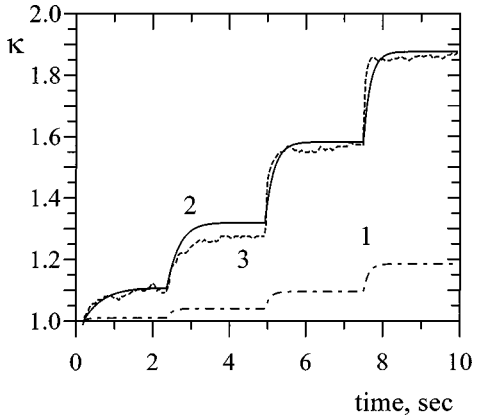

Fig. 3 Comparison of the theoretical elongation kinetics with the experiment: (1) purely shear model; (2) bending-shear model; (3) the curve obtained by processing the measurements (after Ref. 6).

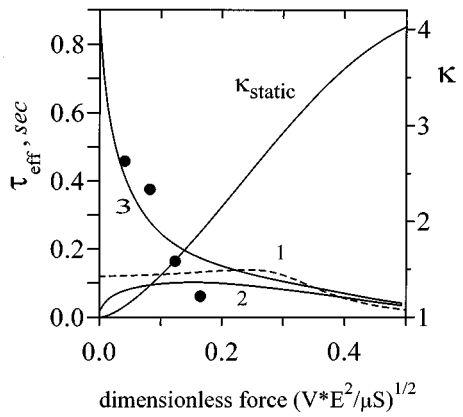

Fig. 4 Variation of the characteristic time of the cell elongation response to the field jump, calculated as a function of the initial field value: (1) purely shear model; (2) bending-shear model with $\tau_1=0$; (3) bending-shear model, $\tau_1/\tau_0=0.3$; κ_{static} is the stationary elongation curve (right vertical scale); $w=110$, $n=0.45$, $\tau_0=0.12$ s. Closed circles: Relaxation time values determined for the stepwise kinetic curve from Ref. 6, processed into curve (3) of Figure 3.

$-E_0| \ll E_0$. As curve 1 shows, the relaxation times calculated using the purely shear model are essentially smaller than the measured ones. According to the general relation $\tau_{\text{eff}} \propto$(viscosity parameter)/(elastic modulus), that means that the purely shear model overestimates the stress that arises during the dynamic deformations. As curve (2) shows, the bending-shear model, neglecting viscous friction in the fluids inside and outside the cell, describes the data measured even more poorly. This is due to a decrease of energy dissipation in the membrane because of reduced shear deformations in the bending-shear model. However, the bending-shear model which gives a proper accounting of viscous friction in the fluids gives the right description of the observed $\tau_{\text{eff}}(E)$ dependence [curve (3)]. The remaining discrepancy has two likely origins. First, the experimental data cited in Ref. 6 are a single elongation recording with a rather high noise level. It was presented in Ref. 6 merely for illustration purposes, and no systematic, statistically validated measurements of $\tau_{\text{eff}}(E)$ were done. Second, the theoretical calculations of $\tau_{\text{eff}}(E)$ were based on several of the approximations discussed above, which may substantially influence the quantitative validity of the results. In particular, the ratio value $\tau_1/\tau_0 = 0.3$ required to describe the experimental data presented in Figures 3 and 4 is substantially larger that the expected from the expressions for τ_1 and τ_0 with $\eta_s = 6\times10^{-7}$ N s/m and $\eta_i = 6\times10^{-3}$ N s/m^2. Another possible reason for the deviation of the theoretical curves from the measured points, especially marked at high cell elongations (last data point in Figure 4), is the nonlinear behavior of the viscosity of the composite membrane material.

5 DISCUSSION AND CONCLUSIONS

The dielectro-deformation technique showed a high sensitivity to variations in the mechanical properties of erythrocytes caused by physical, biochemical, and disease-induced changes in the cell.[6] Combined with the contactless mode and high versatility of the deformation procedures, it makes this technique potentially very advantageous for applications in cell biomechanics and medical diagnostics. However, the physical picture of the dielectro-deformation phenomenon is essentially more complex compared to mechanical deformational processes. It was believed that the principal sources of elastic stress that arise in the course of dielectro deformation of erythrocytes, were the shear deformations of the membrane.[5,6,8,10] One of the most important results of this work is the revision of this concept. It is shown that the dielectro-deformation process of erythrocytes is determined by a combination of bending and shear elastic stresses of comparable strength that arise in the erythrocyte membrane. As a result, the stationary dielectro deformations depend on two elastic moduli of the membrane, bending elastic modulus K_c and shear elastic modulus μ, while the dynamic deformations depend on four moduli: two elastic, K_c and μ, and two viscous, membrane surface viscosity η_s and hemoglobin solution viscosity η_i. Compared to a single parameter μ describing the static, and two parameters, μ and η_s, describing the dynamic deformations reported in previous theories,[5,6,8,10] it means that there are numerous complications in the data evaluation procedures in the dielectro-deformational technique. It also necessitates re-interpretation and re-evaluation of the previously measured data[6,8] regarding the influence of various factors on mechanical moduli.

The bending-shear ellipsoidal model of dielectro deformations of erythrocytes developed in this article allows one to describe both the qualitative features and the quantitative aspect of this phenomenon. Due to analytical formulation, it gives a clear insight into the influence of every group of erythrocyte parameters—mechanical, electric, and geometrical—on cell deformational behavior. A very important point established here is that the electric force influences the deformations not through the field amplitude as such, but through the dimensionless combination $(V/\mu S)^{1/2}E$. That means that precise evaluation of the mechanical parameters of erythrocytes, or even monitoring these parameters under changing conditions, requires knowledge or monitoring of the shape of the cell.

Actually, the problem of incorporating the exact erythrocyte shape into the theory of dielectro deformations becomes much more crucial now. Apart from the dependence of the acting electric force on the transient shape of a deformed cell due to the depolarization effect,[8,10] the cell shape also governs the actual distribution of the bending and the shear deformations in the membrane, hence, the distribution and relative strength of the bending and shear elastic stresses that arise. In the present model this feature was accounted for by a phenomenological relation $\kappa^*(\kappa)$, Eq. (7), between shear deformation of the membrane and cell elongation. The numerical coefficients entering this relation can be determined uniquely from a comparison with the experiment, provided the mechanical moduli of the control cell are known (see Figure 2). This is sufficient for many application purposes. However, the functional form of $\kappa^*(\kappa)$ proper cannot be chosen unambiguously. Actually, a justified choice of this approximation function can be based only on an exact solution of the erythrocyte deformation problem.

Further progress in dielectro-deformational studies of the mechanical properties of erythrocytes and complete realization of the promising potential of this technique requires a more detailed experimental and theoretical study of the dielectro-deformation phenomenon itself.

Acknowledgment

This work was supported by the Russian Foundation for Basic Research under Grant No. 97-04-48855.

REFERENCES

1. N. Mohandas and E. Evans, ''Mechanical properties of the red cell membrane in relation to molecular structure and genetic defects,'' *Annu. Rev. Biophys. Biomol. Struct.* **23**, 787–818 (1994).
2. E. A. Evans and R. Skalak, *Mechanics and Thermodynamics of Biomembranes*, Chemical Rubber Press, Boca Raton, FL (1980).
3. D. Bareford, P. C. W. Stone, N. M. Caldwell, H. J. Meiselman, and J. Stuart, ''Comparison of instruments for measurement of erythrocyte deformability,'' *Clin. Hemorheol.* **5**, 311–322 (1985).
4. R. Bayer, S. Çaglayan, and Jörg Moser, ''Analysis of erythrocyte flexibility by means of laser diffraction: Effects of mechanical stress, photosensitization and ozone,'' in *Static and Dynamic Light Scattering in Medicine and Biology*, R. J. Nossal, R. Pecora, and A. V. Priezzhev, Eds., *Proc. SPIE* **1884**, 291–302 (1993).
5. H. Engelhardt, H. Gaub, and E. Sackmann, ''Viscoelastic properties of erythrocyte membranes in high frequency electric fields,'' *Nature (London)* **307**, 378–380 (1984).
6. H. Engelhardt and E. Sackmann, ''On the measurement of shear elastic moduli and viscosities of erythrocyte plasma membrane by transient deformation in high frequency electric field,'' *Biophys. J.* **54**, 495–508 (1988).
7. H. S. Kage, H. Engelhardt and E. Sackmann, ''A precision method to measure average viscoelastic parameters of erythrocyte populations,'' *Biorheology* **27**, 67–78 (1990).
8. V. L. Kononenko and M. R. Kasymova, ''Forced low-frequency dielectrodeformational oscillations of erythrocytes,'' *Biological Membranes* (Archives of Soviet Science. Life Sciences Section. A cover-to-cover translation of *Biologicheskie Membrany*), Vol. 5, pp. 429–457, Harwood Academic Publishers, Chur, UK (1991).
9. V. L. Kononenko, A. M. Beck, and M. R. Kasymova, ''Dielectro-deformation and flicker spectroscopy: New tools to study mechanical properties of erythrocytes and other cells,'' in *Physical Characterization of Biological Cells*, W. Schütt, H. Klinkmann, I. Lamprecht, and T. Wilson, Eds., pp. 179–188, Verlag Gesundheit GmbH, Berlin (1991).
10. V. L. Kononenko, ''Dielectro-deformational spectroscopy of erythrocytes,'' in *Biochemical Diagnostic Instrumentation*, R. F. Bonner, G. E. Cohn, T. M. Laue, and A. V. Priezzhev, Eds., *Proc. SPIE* **2136**, 163–174 (1994).
11. L. D. Landau and E. M. Lifshits, *Course of Theoretical Physics*, Vol. 8, Electrodynamics of Continuous Media, Pergamon, London (1960).
12. F. Sauer, ''Forces on suspended particles in the electromagnetic field,'' in *Coherent Excitations in Biological Systems*, H. Fröhlich and F. Kremer, Eds., pp. 134–144, Springer-Verlag, Berlin (1983).
13. M. Born and E. Wolf, *Principles of Optics*, Pergamon, Oxford (1964).
14. L. D. Landau and E. M. Lifshits, *Fluid Mechanics*, Pergamon, New York (1959).